

## THEORY OF HADRONIC PRODUCTION OF HEAVY QUARKS\*

C. Peterson<sup>†</sup>Stanford Linear Accelerator Center  
Stanford University, Stanford, California 94305

## ABSTRACT

Conventional theoretical predictions for hadronic production of heavy quarks ( $Q\bar{Q}$ ) are reviewed and confronted with data. Perturbative hard scattering predictions agree qualitatively well with hidden  $Q\bar{Q}$ -production (e.g.,  $\psi, \chi, \Upsilon$ ) whereas for open  $Q\bar{Q}$ -production (e.g.,  $pp \rightarrow \Lambda_C^+ X$ ) additional mechanisms or inputs are needed to explain the forwardly produced  $\Lambda_C^+$  at ISR. It is suggested that the presence of  $c\bar{c}$ -pairs on the 1-2% level in the hadron Fock state decomposition (intrinsic charm) gives a natural description of the ISR data. The theoretical foundations of the intrinsic charm hypotheses together with its consequences for lepton-induced reactions is discussed in some detail.

## 1. INTRODUCTION

One of the most important results recently obtained at the ISR has been the observation of charm with remarkably high cross sections (0.1-0.5 mb) and with momentum distributions indicating diffraction-like production mechanisms.<sup>1-8</sup> This experimental fact is in contradiction with what is expected from hard scattering mechanisms which predict  $\sigma_{c\bar{c}} \sim 50 \mu\text{b}$  at ISR energies with soft  $x_F$ -spectra for the observed charmed particles.<sup>9</sup> (It should be noted however that at SPS and FNAL energies these features of the ISR  $c\bar{c}$ -production has not yet been settled.) As far as hadronic production of hidden charm is concerned (e.g.,  $pp \rightarrow \psi X$ ) the predictions from hard scattering mechanisms seem to be confirmed by experiments.<sup>9</sup> In particular the leading subprocess  $gg \rightarrow P\text{-state} + X$  has been observed explicitly by the

$\hookrightarrow \psi + \gamma$

experimental presence of accompanying photons.<sup>10</sup>

Although the nucleon is usually regarded as a three-quark bound state, its actual Fock state structure in Quantum Chromodynamics is expected to be more complicated. The proton has a decomposition of free Hamiltonian eigenstates<sup>11,12</sup>

$$|uud\rangle, |uudg\rangle, |uudq\bar{q}\rangle, \dots \quad (1)$$

---

\*Work supported in part by the Department of Energy under contract DE-AC03-76SF00515 and by the Swedish National Science Research Council under contract F-PD8207-101.

<sup>†</sup>On leave of absence from NORDITA, Copenhagen, Denmark.

A nonnegligible  $|uudc\bar{c}\rangle$  state in (1) (intrinsic charm) is expected to give fast  $\Lambda_c^+$ 's in hadron-induced reactions since on a long time scale the five constituents should have the same velocity.<sup>13,14</sup>  $\psi$ -production from these  $|uddc\bar{c}\rangle$  states should however be suppressed due to in particular small wavefunction overlap.<sup>14</sup> A Bag calculation<sup>15</sup> of the  $c\bar{c}$ -mixture gives  $P(|uudc\bar{c}\rangle) \approx 1\%$ , which is compatible with the cross section for  $pp \rightarrow \Lambda_c^+ X$  observed at ISR. It is of course crucial and of utmost interest to confront the amount of intrinsic charm with data on leptoproduction. Unfortunately measurement on  $F_2^{\text{charm}}$  from  $\mu^\pm N \rightarrow \mu^\pm \mu^\mp X$  has not yet been performed for high enough  $x_{Bj}$  to provide a crucial test. Some indirect indications of intrinsic charm exist though: The different values of  $\Lambda_{\text{QCD}}$  as measured in  $\mu N$  and  $\nu N$  at high  $Q^2$  can in fact be explained by the onset of charm production which takes place differently in the two reactions.<sup>16</sup> Also for the unexpectedly high rate of observed same sign dimuons in  $\nu$ -reactions the 1% intrinsic charm contributes substantially in the right direction.<sup>14</sup>

This talk is organized as follows: We first (Sect. 2) review the theoretical expectations for heavy quark production starting with estimates for "soft" production mechanisms and then elaborating more on what is expected from perturbative QCD both with regard to hidden and open heavy flavor production. Comparisons with experimental data on  $c\bar{c}$  are found in Sect. 3. In Sect. 4 a general discussion of higher Fock state decomposition of hadronic states is given and in Sect. 5 we argue for the existence of  $|uudc\bar{c}\rangle$  or the 1% level and compute the resulting  $c(x)$  distributions. Hadronic production of charm is discussed in Sect. 6. In Sect. 7 our model for  $c(x)$  is confronted with data from leptoproduction experiments.

## 2. "CONVENTIONAL" THEORETICAL EXPECTATIONS FOR HEAVY QUARK PRODUCTION

The production of heavy quarks in hadronic collisions from soft mechanisms is normally expected to be very suppressed. As an example, when considering hadronic productions of particles as a tunneling phenomena one finds the probability to produce a  $q\bar{q}$  ( $Q\bar{Q}$ )-pair<sup>17</sup>

$$P(q\bar{q}) \sim \exp\left(-\frac{\pi}{\kappa} m_\perp^2\right) \quad (2)$$

where  $m_\perp = \sqrt{p_\perp^2 + m_q^2}$  and  $\kappa$  is the string constant  $\approx 0.2 \text{ GeV}^2$ . Using  $m_u = m_d = 0 \text{ MeV}$ ,  $m_c = 100 \text{ MeV}$ ,  $m_s = 1500 \text{ MeV}$  and  $\langle p_\perp \rangle = 350 \text{ MeV}$  one gets from Eq. (2)

$$u:d:s:c = 1:1:\frac{1}{3}:10^{-10} \quad (3)$$

(The  $s\bar{s}$ -suppression,  $1/3$ , agrees with data in a cascade picture.)

The reason for the strong suppression of  $c$ -quark production is that it is very difficult to localize the energy of a substantial part of a string. Also in other pictures one obtains a strong

suppression. For example in the statistical model<sup>18</sup> approach the probability for D-meson production is given by

$$P \sim \exp(-2m_D/160 \text{ MeV}) \quad (4)$$

which gives the ratio  $\pi:K:D = 1:0.13:3.10^{-5}$ .

However, since large masses are involved one expects that perturbative QCD is applicable. In fact it turns out that the perturbative contribution strongly dominates over the soft one. This is in contrast to, for example, large  $p_{\perp}$ -production where perturbative QCD is only responsible for the fall of the spectrum.

We will divide the discussion of the perturbative QCD predictions into two parts--hidden and open heavy quark production:

#### A. Hidden Heavy Quark Production

Hadronic production of hidden heavy quark pairs, e.g.,  $\psi$ , can take place through the following hard scattering subprocesses<sup>19</sup> (see Fig. 1)

$$q\bar{q} \rightarrow \psi \quad (5a)$$

$$c\bar{c} \rightarrow \psi \quad (5b)$$

$$gg \rightarrow \text{P-state} \rightarrow \chi + \gamma \text{ (or } 3\pi) \quad (5c)$$

$$q\bar{q} \rightarrow \text{P-state} \rightarrow \psi + \gamma \text{ (or } 3\pi) \quad (5d)$$

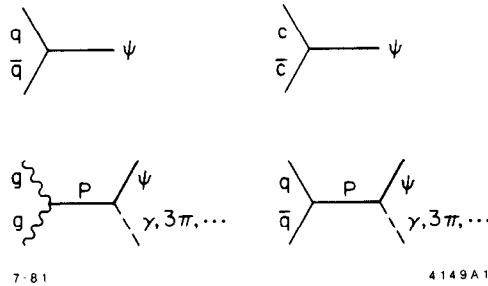


Fig. 1. Lowest order QCD subprocesses for hadron + hadron  $\rightarrow \psi + X$ .

At high energies the gluon-gluon amalgamation process (5c) is the most important due to the abundance of gluons. In the case of  $c\bar{c}$ -production the P-state in Eq. (5c) is  $\chi(3415)$  or  $\chi(3555)$ . The cross section for, e.g.,  $pp \rightarrow \psi X$  with any of the subprocesses above is given by convolution integrals of the type

$$\sigma(pp \rightarrow \psi X) = F \frac{8\pi^2}{M_\chi^3} \Gamma(\chi \rightarrow gg) \iint dx_1 dx_2 G_{g/P}(x_1) G_{g/P}(x_2) \delta(x_1 x_2 s - M_\chi^2) \quad (6)$$

where  $G_{g/P}(x)$  are the gluon (or quark) distributions respectively and  $F$  is an undetermined "fudge"-factor representing uncertainty in color rearrangement, etc.<sup>20</sup>

This hard scattering picture, where the gluon amalgamation process (5c) dominates, is supported by the fact that accompanying photons in connection with  $\psi$ -production have been observed (for details see Ref. 21) with the experimental values<sup>10</sup>

$$B(\chi \rightarrow \psi\gamma) \cdot \frac{\sigma_\chi}{\sigma_\psi} = \begin{cases} 0.70 \pm 0.28 \\ 0.48 \pm 0.21 \end{cases} \quad (7)$$

Furthermore,  $\psi'$ -production seems to be suppressed in hadron-hadron collisions<sup>22</sup> which also supports the  $gg \rightarrow \chi \rightarrow \psi\gamma$  picture since  $m_\chi < m_{\psi'}$ . Also  $\sigma(s)$  and  $d\sigma/dx_F$  from Eq. (6) agrees well with experimental data on  $pA \rightarrow \psi X$  when using gluon distribution<sup>9</sup>

$$G_{g/P}(x) \sim \frac{1}{x} (1-x)^5 \quad (8)$$

Similarly  $T$  production can be fitted by a steeper distribution

$$G_{g/P}(x) \sim \frac{1}{x} (1-x)^6$$

as expected from QCD-evolution.

At lower energies one expects for  $\pi N$  and  $\bar{p}N$ -reactions the  $q\bar{q}$ -subprocesses to be more important. In fact, this is apparent from the  $\bar{p}/p$ -ratio in  $\psi$ -production<sup>23</sup> and the much larger cross section found for  $T$  with pion beams<sup>24</sup> as compared to proton beams at the same energies.

In summary, all the expected features from lowest order graphs Eq. (5) seem to be met by experiment. We now turn to the open charm production.

### B. Open Heavy Quark Production

In the case of open  $Q\bar{Q}$  production the following hard scattering processes contribute<sup>25</sup> (see Fig. 2a,b)

$$q\bar{q} \rightarrow Q\bar{Q} \quad (9a)$$

$$gg \rightarrow Q\bar{Q} \quad (9b)$$

together with the flavor excitation processes<sup>26</sup> (Fig. 2c)

$$qQ(\bar{Q}) \rightarrow qQ(\bar{Q}) \quad (10)$$

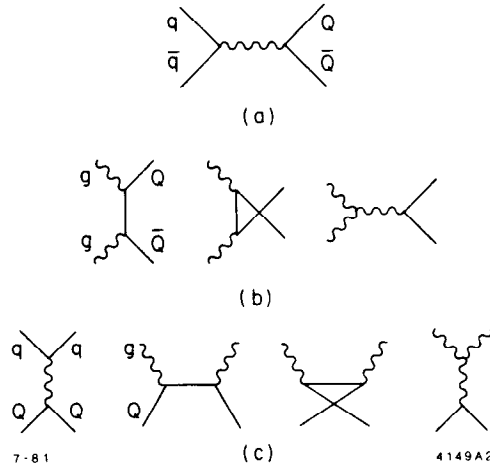


Fig. 2. Lowest order QCD sub-processes for hadron + hadron  $\rightarrow$   $Q\bar{Q} + X$ .

Predictions from the latter ones are uncertain since the heavy quark distribution  $Q(x)$  is not well known.

Again the gluon amalgamation process (9b) is dominant at high energies due to the abundance of low- $x$  gluons. The cross section is given by convolution of distribution functions and the subprocess cross section ( $\hat{\sigma}$ )

$$\sigma(h + h \rightarrow Q\bar{Q}X) = \iint_{x_1 x_2 > x_{\min}} \frac{s_{\min}}{s} dx_1 dx_2 G(x_1) G(x_2) \hat{\sigma}(x_1, x_2, s) \quad (11)$$

Before comparing resulting cross sections and distributions with data on charm, we comment on the theoretical uncertainties entering Eq. (11).

i) The lower limit of Eq. (11). The true kinematical threshold is  $2m_D$  but  $2m_C$  is presumably more relevant since the charmed hadrons are formed in a fragmentation/recombination process, thereby gaining energy.

ii) The value of  $m_C$ . Most authors use  $m_C = 1.6$  GeV. A lower value like  $m_C = 1.2$  GeV, as obtained from potential calculations, would increase the cross section by a factor 4.

iii) Higher order graphs are not yet included.

iv) Higher twist contributions. These are unknown and could be important at such small masses as  $m_C = 1.6$  GeV.

From Eq. (11) the cross section for  $c\bar{c}$  and  $b\bar{b}$ -production in the FNAL (SPS)-ISR energy range is given by (see Fig. 3)

$$\begin{aligned}\sigma(c\bar{c}) &= 1-50 \mu\text{b} \\ \sigma(b\bar{b}) &= 0.1-100 \text{nb}\end{aligned}\tag{12}$$

The energy dependence is logarithmic which is due to the  $1/x$ -behavior of the gluon distributions. The single particle spectrum for the observed charmed hadrons are expected to be soft, reflecting the incoming gluon distributions.

### 3. COMPARISON WITH EXPERIMENTAL RESULTS ON OPEN CHARM PRODUCTION

The experimental results on charm production are reviewed in detail in Ref. 27. Here we only briefly mention the most important results. They are:

- i) At ISR one observes a large cross section (0.1-0.5 mb) for the reaction  $pp \rightarrow \Lambda_c^+ X$  (see Fig. 3b).
- ii) Moreover, the  $\Lambda_c^+$  seems to be produced diffractively in the forward region of phase space (see Fig. 4a,b). At least one of the experiments has an explicit diffractive trigger.<sup>2</sup>
- iii) At SPS/FNAL experiments the situation is not so clear. One experiment with a diffractive trigger,<sup>28</sup>  $\pi^- p \rightarrow D\bar{D}X$ , observes a forwardly oriented single particle spectrum. However, indirect information from beam dump experiments are consistent with the soft  $x_F$ -spectra typical for hard scattering mechanisms.<sup>27</sup>
- iv) Also recently signals from forwardly produced  $\Lambda_b$  at ISR have been reported.<sup>45</sup>

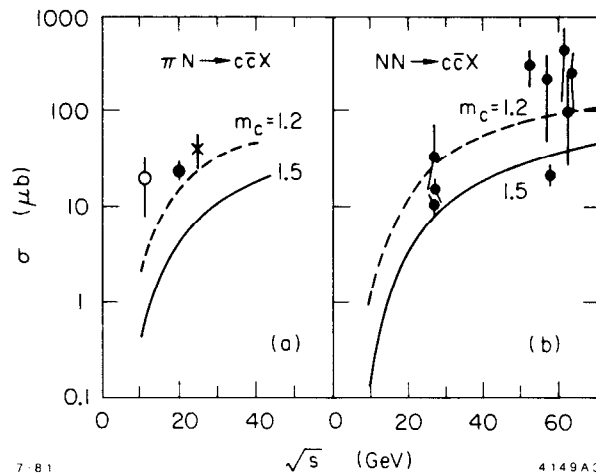


Fig. 3. a)  $\sigma(\pi N \rightarrow c\bar{c}X)$  as a function of c.m.s. energy, from Ref. 9.  
 b)  $\sigma(NN \rightarrow c\bar{c}X)$  as a function of c.m.s. energy, from Ref. 9.

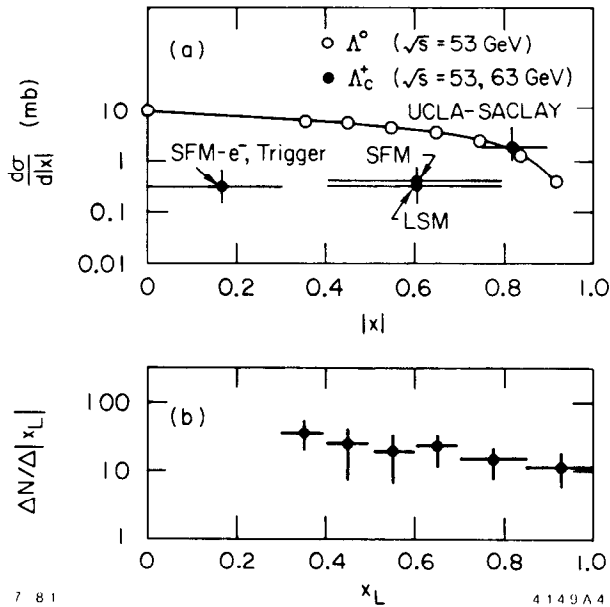


Fig. 4. a)  $d\sigma/d|x|$  for  $\Lambda_c^+$  at 53 and 63 GeV.<sup>1</sup> The smooth curve is a fit to the  $\Lambda^0$  data points. b) Unnormalized  $x_L$ -distribution for  $\Lambda_c^+$  from ref. 8.

Concerning the large cross sections observed at ISR, one could imagine to use a very low value for  $m_c$  [Eq. (11)] ( $m_c = 1.2$  GeV) and thereby approach the ISR data (see Fig. 3). This is however not an attractive solution, since the good agreement of the quark-gluon fusion model with  $\gamma p \rightarrow c\bar{c}X$  data for  $m_c = 1.5$  GeV would then be destroyed.

The other, and more interesting, discrepancy with the hard scattering approach is the  $x_F$ -spectrum of  $\Lambda_c^+$  (see Fig. 4): From general grounds one would expect the  $\Lambda_c^+$  wave function to favor configurations where the c-quarks have the most momentum (see Fig. 5).

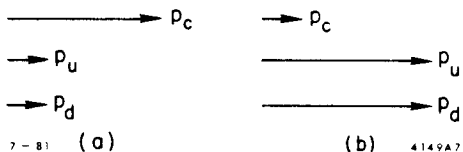


Fig. 5. a) Typical quark momentum configuration in a  $\Lambda_c^+$ . b) Typical quark momentum configuration after a hard scattering with a slow c-quark and two fast valence quarks.

On the other hand, the c-quarks produced in a hard scattering process have small  $x$ . Hence such c-quarks would most unlikely end up in a fast  $\Lambda_c^+$ . It is tempting to conclude that the only way to produce fast  $\Lambda_c^+$  is to have hard  $c(\bar{c})$ -quarks initially present in the proton, i.e.,  $|uudc\bar{c}\rangle$  states.<sup>13,14</sup> We will discuss this intrinsic charm hypothesis in some detail below.

#### 4. HADRONIC FOCK STATE DECOMPOSITIONS

As mentioned in the introduction, the proton has a general decomposition in terms of color singlet eigenstates of the free Hamiltonian. The existence of higher proton Fock states like in Eq. (1) has as far as  $|uudg\rangle$  states some support from hadron spectroscopy: The  $p$ - $\Delta$  mass splitting ( $\Delta E$ ), which is believed to originate from the one gluon exchange graph, is by cutting the diagram in Fig. 6 related to the probability of having extra gluon states,  $P(|uudg\rangle)$ , through the relation

$$\Delta E = \sum_{\substack{\text{gluon} \\ \text{modes}}} P(|uudg\rangle) (E_{uud} - E_{uudg}) \quad (13)$$

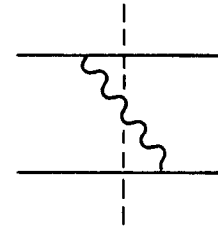
It has also been argued that extra valence gluons are needed in the D-meson in order to explain the  $D^+$  -  $D^0$  lifetime difference. This lifetime difference can be due to the W-exchange graph possible for  $D^0$  (but not  $D^+$ ) provided the helicity suppression is relaxed by the presence of extra valence gluons.<sup>29</sup>

Also in an analysis by Brodsky, Huang and Lepage,<sup>30</sup> it is shown that rigorous constraints from  $\pi \rightarrow \mu\nu$  and  $\pi \rightarrow \gamma\gamma$  decays gives a probability  $< 0.25$  for having a pion in a pure  $q\bar{q}$ -state for a large class of wavefunctions.

In the next section we explore the consequences of heavy quark pairs  $Q\bar{Q}$  in the Fock state decomposition of the bound state wavefunction of ordinary mesons and baryons. Although proton states such as  $|uudc\bar{c}\rangle$  and  $|uudb\bar{b}\rangle$  are surely rare, the existence of hidden charm and other heavy quarks within the proton bound state will lead to a number of striking phenomenological consequences.

It is important to distinguish two types of contributions to the hadron quark and gluon distributions: extrinsic and intrinsic. Extrinsic quarks and gluons are generated on a short time scale in association with a large transverse momentum reaction; their distributions can be derived from QCD bremsstrahlung and pair production processes and lead to standard QCD evolution. The intrinsic quarks and gluons exist over a time scale independent of any probe momentum, and are associated with the bound state hadron dynamics. In particular, we expect the presence of intrinsic heavy quarks,  $c\bar{c}$ ,  $b\bar{b}$ , etc., within the proton state by virtue of gluon exchange and vacuum polarization graphs as illustrated in Fig. 7.

The "extrinsic" quarks and gluons correspond to the standard bremsstrahlung and  $q\bar{q}$  pair production processes of perturbative QCD. These perturbative contributions yield wavefunctions with minimal power-law fall-off



7-81 4149A5

Fig. 6. One gluon exchange diagram responsible for spin-spin splitting of masses and the existence of higher Fock states containing an extra gluon.



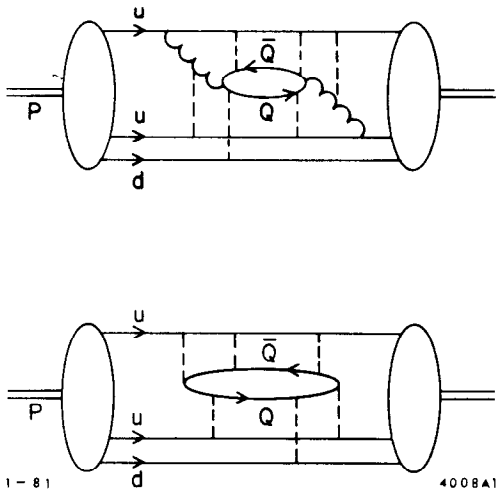


Fig. 7. Diagrams which give rise to the intrinsic heavy quarks ( $Q\bar{Q}$ ) within the proton. Curly and dashed lines represent transverse and longitudinal-scalar (instantaneous) gluons, respectively.

$$|\psi(k_{\perp i}, x_i)|^2 \sim \frac{1}{k_{\perp i}^2} \quad (14)$$

and lead to the logarithmic evolution of the structure functions. In contrast, the intrinsic contributions to the quark distribution are associated with the bound state dynamics and necessarily have a faster fall-off in  $k_{\perp i}$  ( $\psi \sim 1/k_{\perp}^2$  or faster<sup>12</sup>). The intrinsic states thus contribute to the initial quark and gluon distributions. A simple illustration of extrinsic and intrinsic  $|uudq\bar{q}\rangle$  contributions to the deep inelastic structure functions is shown in Fig. 8a and b. We see that existence of gluon exchange graphs, plus vacuum polarization insertions, automatically yield an intrinsic  $|uudq\bar{q}\rangle$  Fock state.

A complete calculation must take into account the binding of the gluon and  $q\bar{q}$  constituents inside the hadron (see Fig. 7) so that the analysis is necessarily non-perturbative.

We also note that the normalization of the  $|uudq\bar{q}\rangle$  state is not necessarily tied to the normalization of the  $|uudg\rangle$  components since the latter only refer to transversely polarized gluons; Fig. 7 shows that  $q\bar{q}$ -pairs also arise from the longitudinal-scalar (instantaneous) part of the vector potential.

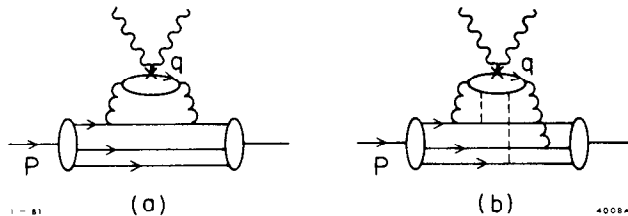


Fig. 8. a) Example with contribution to the deep inelastic structure functions from an extrinsic quark  $q$ .  
b) Example with contribution to the deep inelastic structure functions from an intrinsic quark  $q$ .

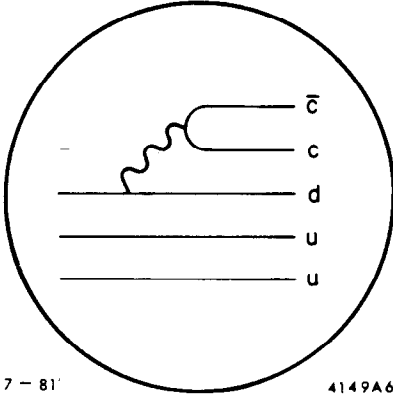
## 5. INTRINSIC HEAVY QUARK STATES

The intrinsic heavy quark states exist on a long time scale. Hence, an estimate of the mixing probability should be possible in the static bag model.<sup>31</sup> Such a study has been done by Donoghue and Golowich<sup>15</sup> in the rest frame of the proton. More precisely they consider states

$$|p\rangle = U(0, -\infty) |p\rangle_0 \quad (15)$$

where  $|p\rangle_0$  is a proton 3-quark state and  $U(0, -\infty)$  is the time development operator in the presence of a QCD interaction

$$U(0, -\infty) = T \exp \left[ -ig \int_{-\infty}^0 dt \int d^3x \bar{\psi}(x) \gamma^\mu \frac{\lambda^a}{2} \psi(x) A_\mu^a(x) \right] \quad (16)$$



To second order in the coupling constant  $g$ , quark pairs are produced according to Eq. (16) via the mechanism in Fig. 9. The probability of a particular  $q\bar{q}$ -component in the proton is obtained by an overlap of the wavefunction (Eq. (15)) with itself. Using bag wavefunctions<sup>31</sup> as inputs in Eq. (16) and summing over the lowest states the authors of Ref. 15 obtain the result

$$\begin{aligned} P(|uudu\bar{u}\rangle) : P(|uudd\bar{d}\rangle) : \\ P(|uud\bar{s}\bar{s}\rangle) : P(|uudc\bar{c}\rangle) \end{aligned} \quad (17)$$

Fig. 9. A  $c\bar{c}$  pair produced by the action of a gluon through the interaction given in Eq. (16).

$$= 0.20:0.15:0.09:0:0.01$$

which, as far as charm is concerned, is in agreement with the order of magnitude of the charm cross section observed at the ISR. It should also be remarked that the results of Eq. (17) are still consistent with previous bag calculations for the static quantities like magnetic moments and average square radii. For our purposes it would be desirable to have the calculation of the intrinsic charm content of the proton performed in the infinite momentum frame. This is presently being investigated.<sup>32</sup>

We now proceed to discuss the  $c$ -quark momentum distribution in a  $|uudc\bar{c}\rangle$  state. The general form of a Fock state wavefunction is

$$\psi(k_{\perp i}, x_i) = \frac{\Gamma(k_{\perp i}, x_i)}{M^2 - \sum_{i=1}^n \left( \frac{m^2 + k_{\perp i}^2}{x} \right)} \quad (18)$$

where  $\Gamma$  is the truncated wavefunction or vertex function. The actual form of  $\Gamma$  must be obtained from the non-perturbative theory, but following Ref. 30 it is reasonable to take  $\Gamma$  as a decreasing function of the off-energy-shell variable

$$\mathcal{E} = M^2 - \sum_{i=1}^n \left( \frac{m^2 + k_{\perp}^2}{x} \right)_i .$$

Independent of the form  $\Gamma(\mathcal{E})$ , we can read off some general features of the quark distributions:

(1) In the limit of zero binding energy  $\psi$  becomes singular and the fractional momentum distributions peak at the values  $x_i = m_i/M$ . More generally,  $\mathcal{E}$  is minimal and the longitudinal momentum distributions are maximal when the constituents with the largest transverse mass  $m_{\perp} = \sqrt{m^2 + k_{\perp}^2}$  have the largest light-cone fraction  $x_i$ . This is equivalent to the statement that constituents in a moving bound state tend to have the same rapidity.

(2) The intrinsic transverse momentum of each quark in a Fock state generally increases with the quark mass. In the case of power law wavefunction  $\psi \sim (\mathcal{E})^{-\beta}$  we have  $\langle k_{\perp}^2 \rangle \propto m_Q^2$ ; for an exponential wavefunction  $\psi \sim e^{-\beta \mathcal{E}^{1/2}}$ , the dependence is  $\langle k_{\perp}^2 \rangle \propto m_Q^2$ .

In the limit of large  $k_{\perp}$  one can use the operator product expansion near the light cone (or equivalently gluon exchange diagrams) to prove that, modulo logarithms, the Fock state wavefunctions fall off as inverse powers of  $k_{\perp}^2$ .<sup>12</sup> For our purpose, which is to illustrate the characteristic shape of the Fock states containing heavy quarks, we will choose a simple power-law form for the Fock state longitudinal momentum distributions

$$P_{(n)}(x_1 \dots x_n) = N_{(n)} \frac{\delta \left( 1 - \sum_{i=1}^n x_i \right)}{\left( M^2 - \sum_{i=1}^n \frac{\hat{m}_i^2}{x_i} \right)^2} \quad (19)$$

where the  $\hat{m}_i^2$  are identified now as effective transverse masses  $\hat{m}_i^2 = m_i^2 + \langle k_{\perp}^2 \rangle_i$  and the  $\langle k_{\perp}^2 \rangle$  are average transverse momentum. With this choice, single-quark distributions have power-law fall-offs  $(1-x)^2$  and  $(1-x)^3$  for mesons and baryons, respectively.

For example, consider a  $|\bar{q}Q\rangle$  state, e.g., a D-meson. Here the momentum distributions of the 2 quarks are according to Eq. (19) given by

$$P(x_1, x_2) = N \frac{\delta(1 - x_1 - x_2)}{\left(m_D^2 - \frac{\hat{m}_c^2}{x_1} - \frac{\hat{m}_u^2}{x_2}\right)^2} \quad (20)$$

From this expression we obtain the charmed quark distribution

$$P(x_1) = \int_0^{1-x_1} P(x_1, x_2) dx_2 = N' \frac{1}{\left(1 - \frac{1}{x_1} - \frac{\epsilon}{1-x_1}\right)^2} \quad (21)$$

where  $N' = N/m_D^4$ ,  $\epsilon = \hat{m}_u^2/m_D^2$  and we take  $m_D^2 \approx \hat{m}_c^2$ . We see from Fig. 10

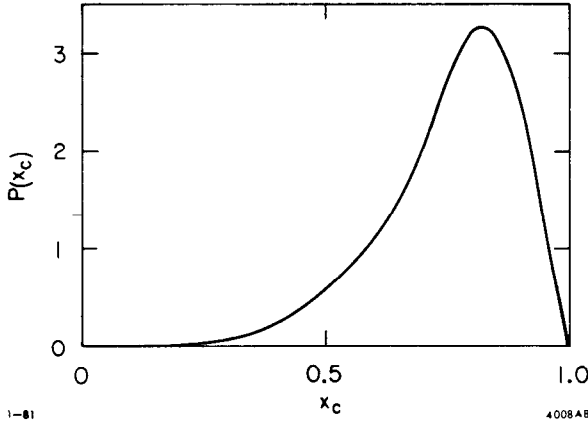


Fig. 10. The  $x$  distribution of the charmed quark in a D-meson.

that the  $c$ -quark tends to carry most of the D-meson momentum ( $\langle x_1 \rangle = 0.73$ ). This leading feature of the  $c$ -quark is due to the fact that the quarks should have roughly the same velocity in order for the hadron to "stay together." This can be seen more explicitly by minimizing the off-shellness, i.e., the denominator in Eq. (20)

$$\frac{\hat{m}_c^2}{x_1} = \frac{\hat{m}_u^2}{x_2} \quad (22)$$

keeping the transverse masses fixed. (A related idea has previously been considered by Bjorken and Suzuki<sup>33</sup> in the context of charm fragmentation into hadrons.)

We now turn to the discussion of  $|uudQ\bar{Q}\rangle$  and  $|u\bar{d}Q\bar{Q}\rangle$  states. For a  $|uudc\bar{c}\rangle$  proton Fock state the momentum distribution is given by

$$P(x_1, \dots, x_5) = N \frac{\delta\left(1 - \sum_{i=1}^5 x_i\right)}{\left(m_p^2 - \sum_{i=1}^5 \frac{\hat{m}_i^2}{x_i}\right)^2} \quad (23)$$

In the limit of heavy quarks  $\hat{m}_4^2 = \hat{m}_5^2 = \hat{m}_6^2 \gg m_p^2$ ,  $\hat{m}_i^2$  ( $i = 1, 2, 3$ ) we get

$$P(x_1, \dots, x_5) = N_5 \frac{x_4^2 x_5^2}{(x_4 + x_5)^2} \delta\left(1 - \sum_{i=1}^5 x_i\right) \quad (24)$$

where  $N_5 = 3600 P_5$  is determined from  $\int dx_1 \dots dx_5 P(x_1, \dots, x_5) = P_5$ , where  $P_5$  is the  $|uudc\bar{c}\rangle$  Fock state probability. Integrating over the light quarks ( $x_1, x_2$  and  $x_3$ ) we get the charmed quark distributions

$$P(x_4, x_5) = \frac{1}{2} N_5 \frac{x_4^2 x_5^2}{(x_4 + x_5)^2} (1 - x_4 - x_5)^2 \quad (25)$$

By performing one more integration we obtain the charmed quark distribution

$$P(x_5) = \frac{1}{2} N_5 x_5^2 \left[ \frac{1}{3} (1 - x_5)(1 + 10x_5 + x_5^2) - 2x_5(1 - x_5) \log \frac{1}{x_5} \right] \quad (26)$$

which has average  $\langle x_5 \rangle = 2/7$  and is shown in Fig. 11. This is to be contrasted with the corresponding light quark distribution derived from Eq. (13) and shown in Fig. 12

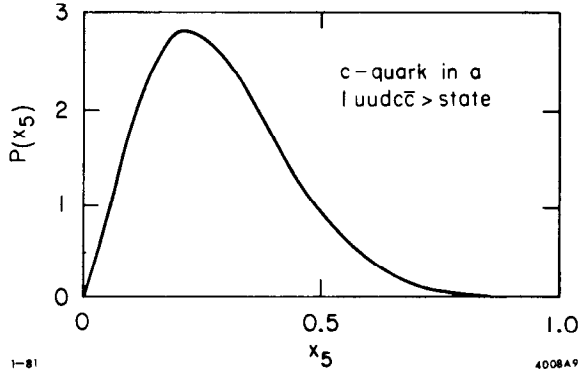


Fig. 11. The  $x$  distribution of the charmed quark in a  $|uudc\bar{c}\rangle$  state.

$$P(x_1) = 6(1 - x_1)^5 P_5 \quad (27)$$

The corresponding  $c$ - and  $u$ -quark distributions in a  $|uudc\bar{c}\rangle$  are obtained in the same way.<sup>14</sup> In order to see the contribution of the intrinsic  $cc$ -pairs to the proton structure function we use the value for  $P_5 = 0.01$  from the bag model calculations discussed above. The magnitude of the charm cross section at ISR (0.1-0.5 mb)<sup>1</sup> gives for  $P_5$ :

$$P_5 = \frac{\sigma_{\Lambda_c}}{2\sigma_{inel}} \approx \frac{250 \mu\text{b}}{2.30 \text{ mb}} = 0.004 \quad (28)$$

If the production mechanism is inelastic and

$$P_5 = \frac{\sigma_{\Lambda_c}}{2\sigma_{diff}} \approx \frac{250 \mu\text{b}}{2.10 \text{ mb}} = 0.01 \quad (29)$$

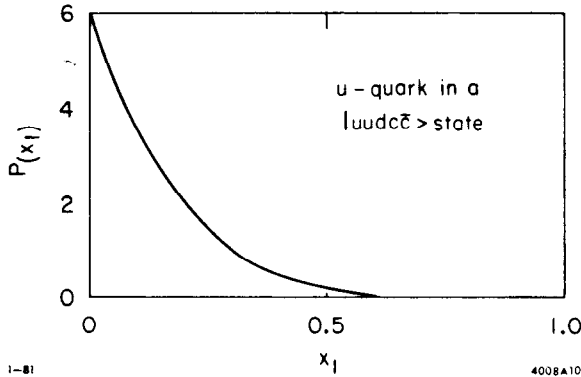


Fig. 12. The  $x$  distribution of a light quark in a  $|uudc\bar{c}\rangle$  state.

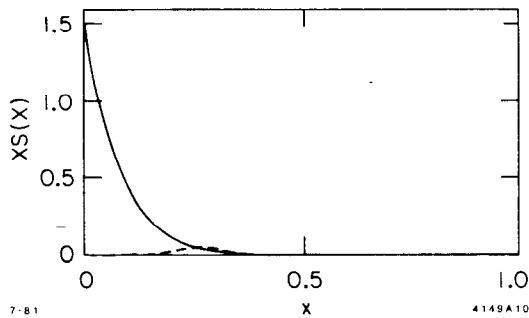


Fig. 13. Comparison of the intrinsic charm sea  $xc(x)$  (dashed line) with the total sea at  $Q^2 = 5 \text{ GeV}^2$  as parametrized by Ref. 34.

if it is diffractive. These two possibilities will be discussed in the next section. We conclude that the charm cross section at ISR is compatible with  $P_5 = 0.01$ .

The charmed quark distribution  $c(x) = P(x_5)$  should be measurable in lepto-production for high enough  $Q^2$  and  $W^2 > W_{th}^2 = 25 \text{ GeV}^2$ . Hence to measure  $c(x)$  at, e.g.,  $x = 0.5$  requires  $Q^2 = 25 \text{ GeV}^2$  ( $x = Q^2/(Q^2 + W^2)$ ). We emphasize that the intrinsic charm sea  $c(x)$  is "rare" but not "wee" as is clear from Fig. 13. A discussion on comparing  $c(x)$  with lepto-production data is found in Sect. 6. In order to obtain intrinsic  $u$ ,  $d$  and  $s$ -distributions ( $|uudu\bar{u}\rangle$  states, etc.) the wavefunction in Eq. (19) needs a minor modification.

## 5. HADRONIC PRODUCTION OF CHARM

Hadronic production of multiparticle final states occurs in two different ways, diffractive dissociation and nondiffractive inelastic production. Although at least one experiment on  $\Lambda_c^+$ -production has an explicit diffractive trigger, the situation for charm production is far from settled. We will discuss the two production mechanisms below in the light of intrinsic charm.

### A. Diffractive Dissociation

Diffractive production of high  $M^2$ -states can be interpreted as a short distance phenomenon due to the large masses involved. Thus perturbative QCD should be applicable to some extent. This idea was first considered in Ref. 35 in the context of charm production. Recently these questions have been studied in more detail for high mass diffraction in general in terms of so-called "transparent states."<sup>36-39</sup> The idea is simple and appealing: when the valence

quarks of a hadron are close together the net color extension is almost zero and the hadron does not interact with other hadrons. Hence the absorptive cross section is small and the hadron scatters diffractively off the target which then appears to be transparent. This situation is, as pointed out by Ref. 37, very similar to an analogous process in QED: when  $e^+e^-$ -pairs are produced in very high energy emulsion experiments, they can only be separated by distances smaller than atomic sizes. The  $e^+e^-$  has net charge zero—it is not "seen" by surrounding atoms and hence it does not ionize and give rise to visible tracks. In Ref. 39 the authors explore the knowledge of the pion wavefunction in QCD at short distances in this context and derive interesting results for the jets emerging from the "transparent" target.

As was discussed in connection with Eq. (18) one expects intrinsic heavy quark states to have large  $\langle p_{\perp} \rangle$  and consequently small transverse dimension. It is therefore tempting to assume that the intrinsic heavy quark states scatter diffractively. With that assumption the authors of Ref. 39 obtain in the case of 1% intrinsic charm on a nuclear target

$$\sigma_{\text{charm}}^{\text{diff}} = 0.01 \cdot \sigma_{e1} \approx 0.5 \text{ mb} \cdot A^{2/3} \quad (30)$$

This high value is encouraging as far as production of b- and t-quarks are concerned. A diffractive production mechanism of heavy quarks is also very favorable as far as the combinatorial background is concerned.

For the charm case the  $\Lambda_c$  and D-spectra can be calculated in principle from the strong overlap between the 5-quark and the charmed-hadron state wavefunctions, allowing for decays of excited state, etc. For the purpose of obtaining the  $x_F$ -distributions we shall use a simple recombination mechanism for the quarks involved in the states. Neglecting its binding energy, the  $\Lambda_c$  spectrum is given by combining the u, d and c-quark in  $|uudc\bar{c}\rangle$  to obtain

$$P(x_{\Lambda_c}) = N_5 \int_0^1 \prod_{i=1}^5 dx_i \delta(x_{\Lambda_c} - x_2 - x_3 - x_4) \left( \frac{x_4 x_5}{x_4 + x_5} \right)^2 \delta \left( 1 - \sum_{i=1}^5 x_i \right) \quad (31a)$$

(see Fig. 14) with  $\langle x_{\Lambda_c} \rangle = 1/7 + 1/7 + 2/7 = 4/7$ . The ISR data for  $d\sigma/dx$  ( $pp \rightarrow \Lambda_c X$ ) (see Fig. 4) are consistent with the prediction from Eq. (31) that charmed baryons are produced in the forward fragmentation region, although the existing data are too scarce for a detailed comparison. We expect that the low x region for charm production will be filled in by both perturbative and higher Fock state intrinsic contributions. The corresponding distribution for  $D^-(\bar{c}d)$  is given by

$$P(x_{D^-}) = N_5 \int_0^1 \prod_{i=1}^5 dx_i \delta(x_{D^-} - x_3 - x_5) \left( \frac{x_4 x_5}{x_4 + x_5} \right)^2 \delta\left(1 - \sum_{i=1}^5 x_i\right) \quad (31b)$$

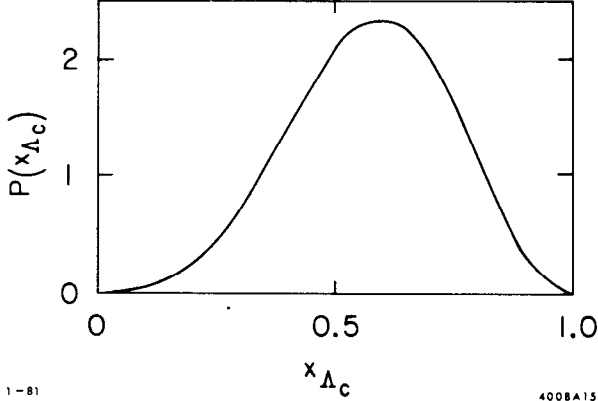


Fig. 14. The  $x$  distribution of the  $\Lambda_c^+$  from the intrinsic charm component of the proton.

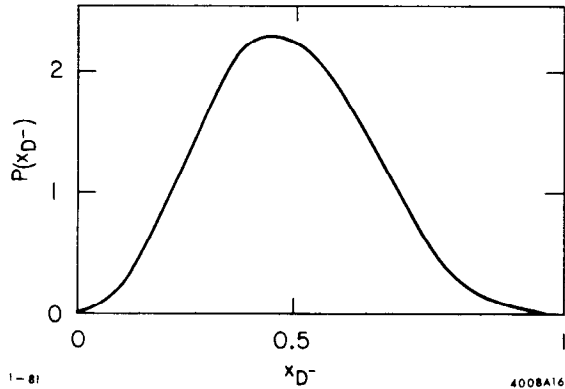


Fig. 15. The  $x$  distribution of the  $D^-$  from the intrinsic charm component of the proton.

with  $\langle x_{D^-} \rangle = 1/7 + 2/7 = 3/7$ , and is shown in Fig. 15. The  $D^+(c\bar{d})$  distribution would, in principle, be obtained from the  $|uudc\bar{c}\bar{d}\bar{d}\rangle$  Fock state of the proton, where the  $\bar{d}\bar{d}$  could be extrinsic or intrinsic. Assuming that the  $\bar{d}$  momentum is small, the  $D^+$  distribution should be close to that of the  $c$ -quark shown in Fig. 11. These predictions apply for forward production ( $x_F \gtrsim 0.1$ ), where perturbative contributions and higher Fock state contributions can be neglected. Spectra for pion induced reactions are obtained in the same way.<sup>14</sup>

In addition to charmed mesons and baryons, the  $J/\psi$  may also be produced diffractively from the intrinsic charm component of the proton. Compared to the charm production cross section at FNAL energies<sup>27</sup>

$$\sigma(\pi N \rightarrow DX) \approx 20 \mu\text{b} \quad , \quad (32)$$

$J/\psi$  production data around 200 GeV give<sup>40</sup>

$$\sigma(\pi N \rightarrow \psi X) \approx 100 \text{ nb} \quad .$$

Further, the observed  $x_F$ -distribution appears to be more strongly peaked near  $x \approx 0$  compared to what would be expected from the intrinsic charm distribution. Evidently most of the  $\psi$  production comes from other central production mechanisms such as gluon and  $q\bar{q}$  fusion.<sup>19</sup> In order for the intrinsic charm model to be consistent, there must be a large suppression factor for the  $\psi$  production from the intrinsic charm compared to the  $D$  production

$$\left. \frac{\sigma(\pi N \rightarrow \psi X)}{\sigma(\pi N \rightarrow DX)} \right|_{\text{intrinsic charm}} \lesssim 5 \times 10^{-5} \quad . \quad (33)$$



In fact, there are a number of factors which act to suppress the production of forward  $\psi$  from the intrinsic charm

(1) In the decay of the  $|uudc\bar{c}\rangle$  state, the probability that the  $\bar{c}$  quark combines to form a  $c\bar{c}$  system is about  $1/4$  (flavor suppression). Similarly, the flavor suppression factor for the  $|udc\bar{c}\rangle$  state is about  $1/2$ .

(2) A  $c\bar{c}$  system can be formed in either a color octet  $c\bar{c}$  or singlet  $c\bar{c}$  state. The color octet  $c\bar{c}$  state should interact with other colored particles and is most likely to decay into open charm particles such as  $\bar{D}$ 's. Therefore, we can take only the color singlet combination of  $c\bar{c}$  for  $\psi$  production. This occurs only  $1/9$  of the time (color suppression).

(3) If the color singlet  $c\bar{c}$  system has a mass larger than the  $D\bar{D}$  threshold, it will decay strongly into charmed particles rather than  $\psi$  production. Therefore, we have to require that the invariant mass  $M_{c\bar{c}}$  is below the  $D\bar{D}$  threshold (mass suppression)

$$2m_c < M_{c\bar{c}} < 2m_D \quad . \quad (34)$$

In Ref. 14 the  $M_{c\bar{c}}^2$ -distribution (see Fig. 16) was calculated from Eq. (25). From that distribution one obtains

$$\int_{4\hat{m}_c^2}^{4m_D^2} dM_{c\bar{c}}^2 \frac{dP}{dM_{c\bar{c}}^2} \approx 10^{-2} \quad . \quad (35)$$

(4) Even if the  $c\bar{c}$  system is below  $D\bar{D}$  threshold, it may be realized as  $\chi$ ,  $\eta_c$  and  $\psi'$  states which do not decay into  $\psi$ 's. We estimate this suppression factor as  $1/3$  (channel suppression). If we combine the factors in (1)-(4) we obtain the very rough theoretical estimate

$$\left. \frac{\sigma(\pi N \rightarrow \psi X)}{\sigma(\pi N \rightarrow DX)} \right|_{\text{intrinsic charm}} \approx 5 \times 10^{-5} \quad . \quad (36)$$

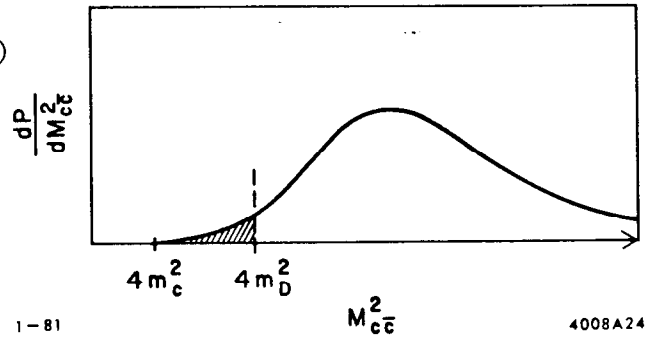


Fig. 16. The  $c\bar{c}$  mass spectrum in the intrinsic charm state  $|uudc\bar{c}\rangle$ . The shaded area corresponds to the  $\chi$ ,  $\eta_c$ ,  $\psi$  and  $\psi'$  production.

Despite these uncertainties, it is clear that although the intrinsic charm model does predict  $\psi$  production in the forward fragmentation region, the rate is at a very suppressed level.

## B. Inelastic Nondiffractive Production

In Ref. 41 a perturbative analysis was carried out using the graphs of Fig. 2c. For the charm quark distribution  $c(x)$  the

authors use essentially that from the intrinsic charm.<sup>47</sup> As is seen from Fig. 17, the final charm x-spectra get contributions from both the spectator c and the one participating in the Fig. 2c subprocess.

We end this section by discussing the energy dependence for heavy quark production.

For perturbative heavy quark production mechanisms,<sup>25</sup> the energy dependence of the cross section essentially comes from the lower limit  $m_Q/(2\sqrt{s})$  of convolution integrals, and gives rise to a logarithmic energy dependence. To study the energy dependence of the "diffraction" mechanism with "intrinsic" heavy quarks we will use the empirical formula for high mass diffraction<sup>48</sup>

$$\frac{d\sigma}{dM^2} = \sigma_0 \frac{1}{M^2} \quad (37)$$

valid for  $M^2 \gtrsim 2 \text{ GeV}^2$ . The integrated charm cross section is given by

$$\sigma = \sigma_0^c \int_{M_0^2}^{M_1^2} \frac{dM^2}{M^2} = \sigma_0^c \log \frac{(1 - x_1)s}{(M_{\Lambda_c} + M_D)^2}, \quad (38)$$

where in this case  $M_0^2$  is the threshold value for associated production of a pair of hadrons containing charmed quarks. The upper limit  $M_1^2$  is determined from the kinematical relation  $M_1^2 = s(1 - x_1)$  where  $x_1$  is the lower fractional momentum cut on the recoiling proton. In the ISR  $pp \rightarrow p_1 \Lambda_c X$  experiment<sup>2</sup> one triggers on events with  $x_1 \geq 0.8$ . If we assume that essentially all the charm cross section  $\sigma_c \sim 300 \mu\text{b}$  is due to diffractive production, then we can determine  $\sigma_0 = 77 \mu\text{b}$ . From this we predict that at SPS and FNAL energies ( $s \cong 400\text{--}600 \text{ GeV}^2$ ), the total  $pp \rightarrow$  charm cross section should be of the order of  $150 \mu\text{b}$ . Clearly this prediction is larger than present experimental data at SPS/FNAL with both pion and proton beams.<sup>27</sup> The energy dependence thus seems to be stronger than what is implied by Eq. (38).

Concerning production of heavy quarks on nuclear targets one expects an  $A^{2/3}$ -dependence from the intrinsic charm model. This is in contrast to the perturbative hard scattering cross section, which should be proportional to  $A$ .

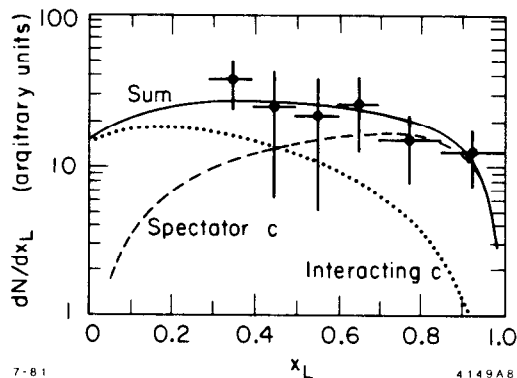


Fig. 17. Longitudinal momentum distributions from Ref. 41 for charm in  $pp \rightarrow c\bar{c}X$  based on the diagrams of Fig. 2c. The input charm distribution is essentially that of the intrinsic charm.

As far as the production of b- and t-quarks are concerned, one can argue on general grounds that the probability of a hadron to contain an intrinsic heavy quark pair should fall as

$$P_{Q\bar{Q}} \propto \frac{\alpha_s^2}{R^2 m_Q^2} \quad (39)$$

where R is a hadron size parameter. Using the same (1-x)-cut as in Eq. (38) and  $m_t = 20$  GeV one obtains the cross sections for b- and t-quark production as shown in Table I.

Table I. Cross section for b- and t-production at ISR and Tevatron energies from Eq. (38) and (39). The numbers in parentheses are the conventional perturbative QCD-predictions.

	ISR ( $\sqrt{s} = 63$ GeV)	Tevatron ( $\sqrt{s} = 2000$ GeV)
b	15 $\mu\text{b}$ (0.5)	70 $\mu\text{b}$ (2)
t ( $m_t = 20$ GeV)	0	3 $\mu\text{b}$ (0.1)

## 7. THE INTRINSIC CHARM AND LEPTOPRODUCTION EXPERIMENTS

As is clear from Fig. 13, the intrinsic charm sea is very small compared to the total sea. However, it should be visible in experiments explicitly looking for lepto-production of charm. This is the case in dimuon production (Fig. 18a)

$$\mu^\pm N \rightarrow \mu^\pm \mu^\pm X \quad (40)$$

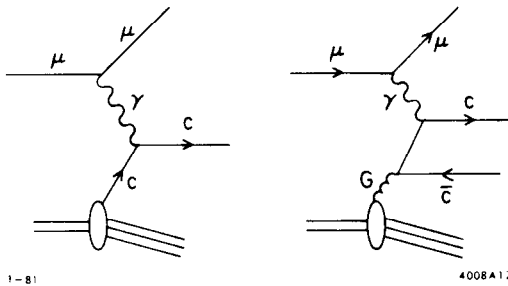


Fig. 18. Lepto-production of charm from the intrinsic charm sea and via the proton-gluon fusion model, respectively.

where one of the final state muons originates from charm decay. However, there exists a competing process with similar experimental signature, photon-gluon fusion<sup>42</sup> (Fig. 18b). The two processes should be additive. Analyses of reaction (40) is somewhat model dependent as far as the charm fragmentation function,  $D_c^D(z, k_\perp^2)$  is concerned. The EMC-collaboration has extracted the charm structure function  $F_2^C$  from the data<sup>43</sup> and the result is shown in Fig. 19. Unfortunately the data only extends to  $x_{Bj} = 0.24$  so it does

not provide a crucial test for intrinsic charm on a 1% level but it is clear from Fig. 19 that the intrinsic charm saturates the highest  $Q^2$  data point. However, at high  $Q^2$  one expects the QCD-evolution to have changed the initial  $c(x)$ -distribution. In fact it turns out that

$$\langle x(200) \rangle_c = \int_0^1 xc(x, Q^2 = 200 \text{ GeV}^2) dx \approx 0.20 \quad (41a)$$

as compared to

$$\langle x(Q_0^2) \rangle_c = \int_0^1 xc(x, Q_0^2) dx = \frac{2}{7} \approx 0.29 \quad (41b)$$

using  $Q_0^2 = (1 + 1.5^2) \text{ GeV}^2$  with  $\Lambda = 0.15\text{--}0.4 \text{ GeV}$ .

Although the intrinsic charm contribution to the total structure function  $F_2$  is small globally, it is substantial at large  $x$  ( $\sim 10\%$  for  $x \approx 0.5$ ). D. P. Roy<sup>16</sup> has used this feature to account for the anomalously small scale breaking ( $\Lambda = 0.1$ ) observed in  $\mu N$ -data without affecting the SLAC-MIT or CDHS results ( $\Lambda = 0.3\text{--}0.4 \text{ GeV}$ ). The idea is the following: The value  $\Lambda = 0.4 \text{ GeV}$  corresponds to a 30% decrease of  $F_2^{\mu N}$  at large  $x$  and  $Q^2 = 20\text{--}200 \text{ GeV}^2$ . Correspondingly  $\Lambda = 0.1 \text{ GeV}$  represents a 20% decrease. Since the charm threshold occurs in  $\mu N$ -reactions for  $Q^2 \gtrsim 20 \text{ GeV}^2$ , the intrinsic charm ( $\sim 10\%$  for  $x = 0.5$ ) increases  $F_2^{\mu N}$  in this region thereby lowering the apparent value of  $\Lambda$ . (In the  $F_2^{\nu N}$ -case this effect is very small since (1) only half of the charm quarks are excited, and (2) the rise occurred already at  $Q^2 < 20 \text{ GeV}^2$ ). The amount of intrinsic charm required to account for the discrepancy between  $\mu^-$  and  $\nu$ -experiments for different values of  $\Lambda$  is shown in Table II.

A very interesting implication of intrinsic charm for  $\nu N$  and  $\bar{\nu} N$  charge current reactions is the production of beauty quarks ( $\bar{\nu} c \rightarrow \mu^+ b$  and  $\nu c \rightarrow \mu^- b$ ).<sup>14</sup> The subsequent leptonic decay of the  $b$  and  $\bar{b}$  then leads to same-sign muon pairs (see Fig. 20). The experimentally observed rate of same-sign muon pairs is unexpectedly high, although the different experiments do not all agree.<sup>44</sup> The  $c \rightarrow b$  process

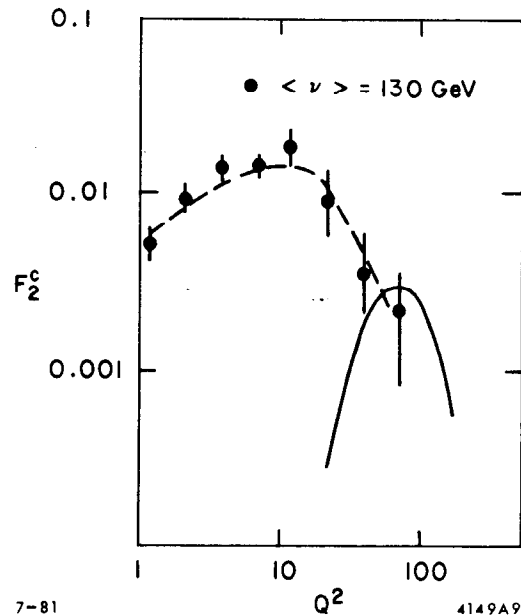


Fig. 19.  $F_2^c(\nu, Q^2) = xc(x, Q^2)$  as extracted from  $\mu N \rightarrow \mu \mu X$  in Ref. 43. The full curve is the expected contribution from intrinsic charm and the dashed curve is the prediction from the photon-gluon fusion model with  $\alpha_s = 0.42$ .

Table II. QCD induced decrease of  $F_2^{\mu N}$  ( $x = .5, Q^2$ ) over  $Q^2 = 20 \rightarrow 200$ , for various values of  $\Lambda$ . Also shown are the corresponding magnitudes of the intrinsic charm component, required to reproduce a net decrease of 20%, as observed by EMC.

$\Lambda(\text{GeV})$	.10	.17	.25	.32	.4
$\frac{F_2(20) - F_2(200)}{F_2(20)}$	19.6%	22.4%	25%	27%	29.4%
Required size of the intrinsic charm component	0%	0.5%	1%	1.5%	2%

works in the right direction, but with present limits on the standard left-handed c-b coupling the theoretical prediction from intrinsic charm is below some experimental data. However, in the context of topless models right-handed couplings,  $(c,b)_R$ , have been suggested which increases the same sign dimuon production from the intrinsic charm.<sup>46</sup>

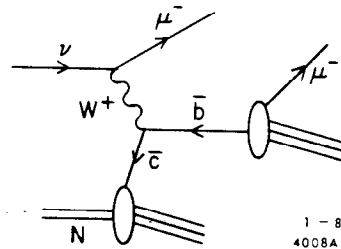


Fig. 20. Same sign dimuon pair production from the intrinsic charm component of nucleons.

## 8. CONCLUSIONS

We conclude with the following remarks:

- Perturbative QCD with conventional inputs works well for hidden heavy quark production (e.g.,  $\psi, T$ ). The dominant subprocess is gluon-gluon fusion.
- For open heavy quark production the predictions from perturbative QCD are in conflict with, in particular, data on  $pp \rightarrow \Lambda_c^+ X$ .
- It is found that higher Fock  $c\bar{c}$ -states in the proton on the 1% level, as suggested by bag model calculations, gives a natural explanation of the open charm production data.
- These intrinsic charm states,  $|uudc\bar{c}\rangle$ , are believed to have small transverse extension. Hence they could materialize diffractively in the context of "transparent states."
- Since the intrinsic heavy quark states scale with  $m_0^2$  one expects nonnegligible cross sections for hadronic production of b- and t-quarks. Furthermore, in diffractive configurations the combinatorial background is less serious than the central collision processes.

Much more theoretical and experimental work is needed, in particular:

- Better understanding of higher Fock states in general; perform refined calculation in the bag model in infinite momentum frame.
- Is charm produced diffractively or not?
- Measurement of  $c(x)$  at large  $x_{Bj}$  in lepton production experiments.
- More experimental study of charm production in the FNAL/SPS energy region.

#### ACKNOWLEDGEMENT

Part of this work was done in collaboration with S. J. Brodsky, P. Hoyer and N. Sakai. I would like to thank the organizers of this meeting for their kind hospitality. I have also benefitted from conversations with M. Barnhill and C. Heusch.

#### REFERENCES

1. For a review, see S. Wojcicki, SLAC-PUB-2603; A. Kernan, Proc. Photon-Lepton Conf. at Fermilab, 1979, p. 535.
2. K. L. Giboni et al., Phys. Lett. 85B, 437 (1979) and A. Kernan, private communication.
3. D. Drijard et al., Phys. Lett. 81B, 250 (1979); W. Geist, Proc. of the Topical Workshop on Forward Production of High-Mass Flavors at Collider Energies, College de France, Paris, 1979.
4. W. Lockman et al., Phys. Lett. 85B, 443 (1979).
5. D. Drijard et al., Phys. Lett. 85B, 452 (1979).
6. F. Muller, in High Energy Physics-1980, proceedings of the XXth Int. Conf. on High Energy Physics, Madison, Wisconsin, edited by L. Durand and L. G. Pondrom (AIP, New York), 1981.
7. A. Chilingarov et al., Phys. Lett. 83B, 136 (1979).
8. M. Basile et al., Nuovo Cimento Lett. 30, 481 (1981); ibid 30, 487 (1981).
9. For a review, see R. Phillips, in High Energy Physics-1980, proceedings of the XXth International Conference on High Energy Physics, Madison Wisconsin, edited by L. Durand and L. G. Pondrom (AIP, New York), 1981.
10. T.B.W. Kirk et al., Phys. Rev. Lett. 42, 619 (1979).
11. The states are defined at equal  $\tau = t + z$  in the light-cone gauge  $A^+ = A^0 + A^3 = 0$ .
12. S. J. Brodsky and G. P. Lepage, Phys. Rev. D22, 2157 (1980) and S. J. Brodsky, Y. Frishman, G. P. Lepage, and C. Sachrajda, Phys. Lett. 91B, 239 (1980), and references therein.
13. S. J. Brodsky, P. Hoyer, C. Peterson, and N. Sakai, Phys. Lett. 93B, 451 (1980); P. Hoyer, in High Energy Physics-1980, proceedings of the XXth International Conference, Madison, Wisconsin, edited by L. Durand and L. G. Pondrom (AIP, New York), 1981.
14. S. J. Brodsky, C. Peterson and N. Sakai, Phys. Rev. D23, 2745 (1981).

15. J. F. Donoghue and E. Golowich, Phys. Rev. D15, 3421 (1977).
16. D. P. Roy, Tata Institute Preprint, Phys. Rev.Lett.47, 213 (1981).
17. For a more detailed discussion, see C. Peterson, proceedings of the Topical Workshop on Forward Production at High-Mass Flavors at Collider Energies, College de France, Paris (1979).
18. See R. Hagedorn, Report No. CERN 71-12.
19. See, e.g., M. B. Einhorn and S. D. Ellis, Phys Rev. D12, 2007 (1975); C. E. Carlson and R. Suaya, ibid. 18, 760 (1978).
20. See, e.g., Ref. 9.
21. See Raja's talk at this conference.
22. B. C. Brown et al., FERMILAB-77/54-EXP.
23. M. J. Corder et al., Phys. Lett. 68B, 96 (1977).
24. L. Camilleri, proceedings of The 1979 International Symposium on Interactions of Leptons and Photons at High Energies (Fermilab).
25. H. Fritzsch, Phys. Lett. 67B, 217 (1977). F. Halzen, Phys. Lett. 96B, 105 (1977). L. M. Jones and H. W. Wyld, Phys. Rev. D17, 759, 1782, 2332 (1978). M. L. Gluck and E. Reya, Phys. Lett. 79B, 453 (1978), 83B, 98 (1979). M. Gluck, J. F. Owens, and E. Reya, Phys. Rev. D17, 2324 (1978). J. Babcock, D. Sivers and S. Wolfram, Phys. Rev. D18, 162 (1978). C. E. Carlson and R. Suaya, Phys. Rev. D18, 760 (1978); Phys. Lett. 81B, 329 (1979); H. Georgi et al., Ann. Phys. 114, 273 (1978); K. Hagiwara and T. Yoshino, Phys. Lett. 80B, 282 (1979); J. H. Kuhn, Phys. Lett. 89B, 385 (1980); J. H. Kuhn and R. Ruckl, MPI-PAE/pTH 7/80; V. Barger, W. Y. Keung and R.J.N. Phillips, Phys. Lett. 91B, 253, 92B, 179 (1980); Z. Phys. C, to be published; Y. Afek, C. Leroy and B. Margolis, Phys. Rev. D22, 86, 93 (1980); M. Gluck, E. Hoffmann and E. Reya, DO-TH 80/13.
26. B. L. Combridge, Nucl Phys. B151, 429 (1979).
27. R. Ruchti's talk at this conference.
28. L. J. Koester, in High Energy Physics-1980, proceedings of the XXth International Conference, Madison, Wisconsin, edited by L. Durand and L. G. Pondrom (AIP, New York, 1981); D. E. Bender, Ph.D. thesis, 2980, University of Illinois (unpublished); J. Cooper, proceedings of the XVth Rencontre de Moriond, 1981 (unpublished).
29. H. Fritzsch and P. Minkowski, Phys. Lett. 90B, 455 (1980).
30. S. J. Brodsky, T. Huang and G. P. Lepage, SLAC-PUB-2540; T. Huang, in High Energy Physics-1980, proceedings of the XXth International Conference, Madison, Wisconsin, edited by L. Durand and L. G. Pondrom (AIP, New York, 1981).
31. A. Chodos, R. Jaffe, K. Johnson, C. Thorn and V. Weisskopf, Phys. Rev. D9, 3471 (1974); T. de Grand, R. Jaffe, K. Johnson and J. Kiskis, Phys. Rev. D12, 2060 (1975).
32. M. Barnhill, private communication.
33. M. Suzuki, Phys. Lett. 71B, 139 (1977); J. D. Bjorken, Phys. Rev. D17, 171 (1978).
34. A. J. Buras and K.J.F. Gaemers, Nucl. Phys. B132, 249 (1978).
35. G. Gustafson and C. Peterson, Phys. Lett. 67B, 81 (1977).
36. J. F. Gunion and D. E. Soper, Phys. Rev. D15, 2617 (1977).
37. J. Pumplin and E. Lehman, Zeitschrift für Physik C9, 25 (1981).

38. G. Gustafson, LUTP 81-1, talk given at the "IXth International Winter Meeting on Fundamental Physics," Siguenza, Spain, February 1981.
39. G. Bertsch, S. J. Brodsky, A. S. Goldhaber and J. F. Gunion, SLAC-PUB-2748; see also the talk by J. F. Gunion at this conference.
40. J. Badier et al., Proc. Lepton-Photon Conf. at Fermilab, 1979, p. 161; CERN/EP 79-61.
41. V. Barger, F. Halzen and W. Y. Keung, University of Wisconsin preprint, DEO-ER/00881-211.
42. J. P. Leveille and T. Weiler, Nucl. Phys. B147, 147 (1979).
43. C. H. Best, Proc. of XVIth Rencontre de Moriond, 1981.
44. T. Y. Ling, proceedings of v'81 International Conference on Neutrino Physics and Astro Physics.
45. M. Basile et al., Nuovo Cimento Lett. 31, 97 (1981).
46. V. Barger, W. Y. Keung and R.J.N. Phillips, Phys. Rev. D24, 244 (1981).
47. Note however that in ref. 41 it is hypothesized that the hard  $c(x)$ -distribution is of perturbative origin and not intrinsic. This is unrealistic since the time-scale involved at  $Q^2 \approx m_c^2$  is too short to allow for the produced  $c$ -quarks to equalize the velocity with the valence quarks thereby providing a hard  $c(x)$ -spectrum. (From deep inelastic ep-experiments it is known that long time-scale bound state effects are not important already at  $Q^2 \approx 1 \text{ GeV}^2$ ).
48. M.G. Albrow et al., Nucl. Phys. B108, 1 (1976).